Available online at www.sciencedirect.com
ScienceDirect
Ceramics International 36 (2010) 2351–2358
CERAMICS INTERNATIONAL
www.elsevier.com/locate/ceramint

Sintering of surfactant modified ZnO–Bi_2O_3 based varistor nanopowders

S. Anas [a], R. Metz [b,c], M.A. Sanoj [a], R.V. Mangalaraja [d], S. Ananthakumar [a,*]

[a] *Materials and Minerals Division, National Institute for Interdisciplinary Science and Technology (NIIST), Council of Scientific and Industrial Research (CSIR), Trivandrum 695019, Kerala, India*
[b] *Institut Charles Gerhardt Montpellier, UMR 5253 CNRS, Université Montpellier 2, ENSCM, 8, rue de l'Ecole Normale, 34296 Montpellier Cedex 05, France*
[c] *Laboratoire Matériaux Energétiques et Composés Polyazotés, Lyon1-CNRS-Isochem (groupe SNPE), UMR 5179 CNRS/UCBL/CNES/SNPE, Université Claude Bernard - Lyon 1, Batiment Berthollet, 69622 Villeurbanne Cedex, France*
[d] *Department of Engineering Materials, University of Concepcion, Chile*

Received 15 March 2010; received in revised form 17 April 2010; accepted 7 June 2010
Available online 3 August 2010

Abstract

Surfactant modified nano-origin ZnO–Bi_2O_3 varistor powder was prepared in presence of cetyltrimethyl ammonium bromide (CTAB) surfactant through an aqueous reflux reaction at 100 °C. The compacted varistor discs made from the nano-origin powders were subjected to step-sintering, microwave sintering and solid-state sintering. The influences of CTAB in different sintering methods were analyzed from the densification characteristics, evolution of sintered microstructures and associated varistor properties (*I–V*). The conventional solid-state sintering produced 96% theoretical sintered dense samples at 1100 °C. The step and microwave sintered samples showed 93% and 99% sintered densities, respectively, with controlled microstructures having grain sizes in the range of 2–6 μm at the given conditions. The CTAB advantages were clearly seen in grain structuring and grain boundary properties, in addition to the enhanced densification and homogenous microstructures for obtaining high breakdown voltage and non-linearity coefficient.

Keywords: Sintering; Nanocrystalline powder; Surfactant; Microstructure; ZnO varistor

1. Introduction

Development of next generation high-energy ZnO varistors such as nanostructured multilayered thin/thick film varistor tapes, flexible ZnO–polymer composite varistors, directionally grown ZnO nano-grained bulk varistors are being attempted using the concepts of nanotechnology [1,2]. Industrial manufacturing of 'nano-grained' varistors, four-fold increase in the energy handling efficiency, drastic reduction in the physical dimensions, a single varistor component weight and minimizing of the solid electronic wastes are a few targets fixed for the future varistor devices. In fact the concept of 'nano-varistors' is widely agreed because they have more number of active ZnO grains and grain boundaries which can yield large current carrying capacity [3,4]. According to Eq. (1), the threshold or breakdown voltage [V_b] is determined by the average grain size [V_g] of the sintered ZnO.

$$V_b = n\,Vg = \frac{D * Vg}{d} \tag{1}$$

where "D" is the electrode spacing, "d" is the ZnO grain size and "V_g" is the voltage per ZnO grain which is estimated as ~3 V [5]. This then implies that tailoring the device breakdown voltage, V_b, is a matter of having an appropriate number of ZnO grains, precisely, varistor equivalent circuits, in series between the electrodes. This condition is easily satisfied by nano-grained varistor microstructures.

Preparation of 'nano-origin' varistor powders and nearly 'zero grain-growth sintering' are the challenges associated with 'nano-grained' varistors. Nano-origin varistor powders with high degree of homogeneity in dopant distribution have been attempted through a variety of chemical techniques like precipitation, combustion, hydrothermal, high-energy ball milling and sol–gel [3–8]. Varistor nanoparticles ranging

* Corresponding author. Tel.: +91 471 2515289; fax: +91 471 2491712.
E-mail address: ananthakumar70@gmail.com (S. Ananthakumar).

0272-8842/$36.00
doi:10.1016/j.ceramint.2010.07.017

between 25 and 50 nm with specific surface areas, in the range of 20–30 m^2/g, were successfully obtained in most of these techniques. It is evident from the reports that the synthesis of size controlled varistor nanoparticles is given more emphasis than the densification of such varistor nanoparticles. Moreover, in many cases an intermediate calcination at <600 °C is often used for the conversion of nano-precursors to fully crystalline ZnO varistor powders. Undoubtedly, it accelerates the particle growth and destroys the nano-nature. Hence, methods for the direct-formation of nanocrystalline ZnO needs to be explored. Nanocrystalline 'core–shell' varistor particles were earlier reported by Suresh C. Pillai et al. where an average grain size of 1.5 μm was achieved at 1050 °C along with a V_b value of 850 ± 30 V/mm [9]. Nano-grained ZnO varistor for high voltage applications has also been achieved through a simple 'solution-coating' technique [10]. On the other hand Rao and co-workers used a spray pyrolysis technique to prepare varistor nanoparticles with size in the range of 20–200 nm [11].

Densification of nano-origin varistor powders without any considerable grain growth still remains as a technical challenge for obtaining nano-grained varistors. Since the non-linearity strongly depends on the density of the varistors, it is important to achieve a sintered density close to the theoretical value of 5.6 g/cm^3 and therefore a sintering temperature of above 1000 °C is definitely required. Though nanoparticles are known to densify at low temperatures, the high surface area of nanoparticles and the presence of multiple varistor forming additives and dopants [Bi_2O_3, Cr_2O_3, MnO_2, BaO, TiO_2, PbO, and SiO_2] increases the tendency of spontaneous grain growth, even at 1000 °C [12,13]. Laser sintering, spark plasma sintering and hot pressing have been attempted to arrest the grain growth during densification [14,15]. However, the high initial investments required limit their application in industries. The presence of surfactant in varistor have been not well attempted earlier for the refinement in varistor properties and in the present work, we compare the sintering of surfactant modified ZnO varistor nanopowders achieved through two-stage sintering, microwave sintering and conventional solid-state sintering techniques. The evolution of microstructures with respect to different modes of sintering is monitored and the varistor properties of the sintered blocks were evaluated. The advantage of using surfactant molecules in the synthesis of varistor nanopowders is also explored and the properties are compared with the control samples prepared without the aid of the surfactant.

2. Experimental

2.1. Synthesis of varistor nanopowders

Zinc nitrate hexahydrate (Merck, 99%), metal nitrates of bismuth (Merck, 99%), cobalt (CDH, 99%) and chromium (CDH, 98%) and antimony chloride (S.D. Fine Chemicals, 98%) were used as the raw materials for synthesis. Cetyltriethylammoniumbromide (CTAB) ($C_{19}H_{42}BrN$, S.D. Fine Chemicals, 98%) was used as the surfactant. Ammonia solution (40%) and nitric acid (16N) were used for controlling the pH. Distilled water was used as the refluxing medium.

The varistor composition containing 94 mol% ZnO, 3 mol% Bi_2O_3 and 1 mol% each of Cr_2O_3, CoO and Sb_2O_3 was chosen for the study. The detailed processing steps involved in the synthesis are already published [16]. Briefly, the varistor precursors were hydrolyzed at pH 8.5 and the precipitate ultrasonically dispersed in isopropanol medium. The reaction mixture, taken in an RB flask was heated gently with the dropwise addition of 0.02 M CTAB. The solution was then refluxed at 100 °C for 2 h. The refluxed product was collected by centrifugal filtration and washed with hot water and isopropanol to remove the excess surfactant. The same synthesis procedure was followed to obtain the control samples, but without the addition of CTAB. All the varistor powders were dried at 70 °C for 6 h.

2.2. Sintering of ZnO varistor nanopowders

Varistor discs with dimensions 13 mm diameter and 2 mm thickness was fabricated by uni-axial pressing at a pressure of 80 MPa. The sintering was achieved through three different modes, namely conventional solid-state, two-stage step and microwave sintering. The details of the sintering conditions are presented in Table 1. The solid-state and step-sintering was performed in an electrically heated silicon carbide furnace. The heating rate was controlled using Libratherm temperature programmer. In case of step-sintering, the sintering temperature was first raised to 1100 °C at a heating rate of 35 °C/min and then the samples were held at that temperature for 10 min to attain equilibrium. Subsequently the temperature was minimized to 850 °C and then soaked for 3 h. Microwave sintering

Table 1
Details of heating cycle used for the sintering of nanocrystalline varistor powder.

Surfactant	Sintering process	Abbreviated sample name	Ramp
With CTAB Without CTAB	Sintering 850 °C	WS 850 WOS 850	3 °C/min up to 250 °C, 5 °C/min up to 600 °C, 8 °C/min up to 850 °C. Soaking for 3 h
With CTAB Without CTAB	Sintering 1100 °C	WS 1100 WOS 1100	3 °C/min up to 250 °C, 5 °C/min up to 600 °C, 8 °C/min up to 1100 °C. Soaking for 2 h
With CTAB Without CTAB	Step-sintering 1100–850 °C	WSS WOSS	35 °C/min up to 1100 °C, 10 °C/min up to 850 °C. Soaking for 3 h
With CTAB Without CTAB	Microwave sintering	WMS WOMS	250 W (20 min), 900 W (20 min)

was performed using a 4 kW, 2.45 GHz microwave furnace. An IR-sensor was used for monitoring the sample temperature. In all the cases cooling was performed at normal cooling rates.

2.3. Characterizations

Crystal structure and phase analysis was done based on X-ray diffraction data (Model: Philips, X'Pert Pro, CuKα radiation, λ = 0.154 nm) between the scanning angles, 2θ = 20–60°. The primary crystallite size was calculated using the Scherrer's equation:

$$\text{crystallite size} = \frac{0.9\lambda}{B\cos\theta} \quad (2)$$

where λ = X-ray wave length, θ = Bragg angle and B = line broadening. The value B is usually measured from the increased peak width at half the peak height, which is derived from Warren formula, $B^2 = B_M^2 - B_S^2$, where B_M is the measured peak width and B_S is the corresponding width of the peak of a standard commercial ZnO powder. A Malvern zeta sizer was used to obtain the particle size distribution (PSD). The average poly-dispersity index (PDI) for the measurement was 0.32. The bulk surface area was determined by the BET technique using a Micromeritics Gemini 2370 instrument operating at liquid nitrogen temperature. Degassing of the samples was done at 200 °C/2 h. The particle morphology was investigated using Scanning Electron Microscopy (JEOL 5600 SL) and Transmission Electron Microscopy (TEM-JEOL JEM 2000X). Thermo Gravimetric Analysis and Differential Thermal Analysis TG/DT-50 H (SHIMADZU, Japan) were performed at a constant heat flow of 10 °C/min in air. The thermal analysis was carried out up to 1200 °C. The sintered microstructure was taken on the fractured surfaces using SEM. The average grain size was determined from the SEM micrographs by an image analysis program. More than 300 grains were taken into account for determining the average grain size. Densities of sintered samples were measured using the Archimedes method.

2.4. Electrical measurements

Varistor properties were evaluated from the standard current–voltage (I–V) measurements. Measurements were performed using a pulsed mode d.c. power supply with built-in power up to 800 V (DIGITRONICS, India) and a current limit of about 100 mA. The dense varistor discs were polished using metallographic grade emery sheet to a thickness to 1 mm. The sintered samples had roughly 12 mm diameter. The samples were electroded with silver and heated at 600 °C for 10 min. The current passing through the cross-section of the sample was monitored for every 10 V and then plotted against current density and electric field. From the I–V curves, the breakdown voltage (V_b) and the non-linearity coefficient (α) were determined. The 'α' value was measured between the current densities of 0.1–1 mA using the relationship: $\alpha = (\log I_2 - \log I_1)/(\log V_2 - \log V_1)$ where V_2 and V_1 are the voltage at current I_2 and I_1.

3. Results and discussions

3.1. Characterization of nanocrystalline varistor powder

Fig. 1 presents the XRD patterns obtained for the nano-origin ZnO varistor powders prepared with and without CTAB. The XRD pattern of the samples prepared without CTAB corresponds to the hexagonal wurtzite phase of ZnO (JCPDS file no. 89-1397) showing its direct crystallization at 100 °C. The samples prepared with CTAB at identical reflux conditions exhibit a broad peak between the 2θ values 30–36° indicating the formation of Zn-nuclei and its amorphous nature. The nucleation and one directional growth of ZnO nanocrystals in the absence of surfactant molecules have been observed under hydrothermal and reflux reactions even below 100 °C at very low concentrations, high pH and extended reaction times [16,17]. The direct-formation of ZnO is hindered in the presence of CTAB due to the capping effect of the surfactant molecules [18]. The adsorbed CTAB layer on the surface of hydroxyl metal-oxide precipitates acts as an interfacial barrier to the diffusion assisted growth of crystalline ZnO. The presence of adsorbed CTAB molecules can be observed in the TG curves given in Fig. 2. The thermogram shows two-step decomposition with significant weight loss in the second step observed between the temperatures 200 and 400 °C. This weight loss corresponds to the decomposition of CTAB and conversion of metal hydroxides to stable crystalline ZnO. CTAB decomposition is generally observed in the temperature range of 220–350 °C [19]. The TG analysis clearly indicates that at least 400 °C is required to obtain crystalline ZnO. A calcination treatment at 500 °C was employed for the as-prepared powders. The XRD pattern of the calcined sample confirm the formation of fully crystalline varistor grade ZnO powders.

Since there is no surfactant and additional calcination treatment involved, the direct-formation route may appear more attractive. The benefit of the surfactant aided synthesis lies in the nano-nature of the resultant particles. Surfactant molecules play significant role in controlling the nucleation kinetics, direction of

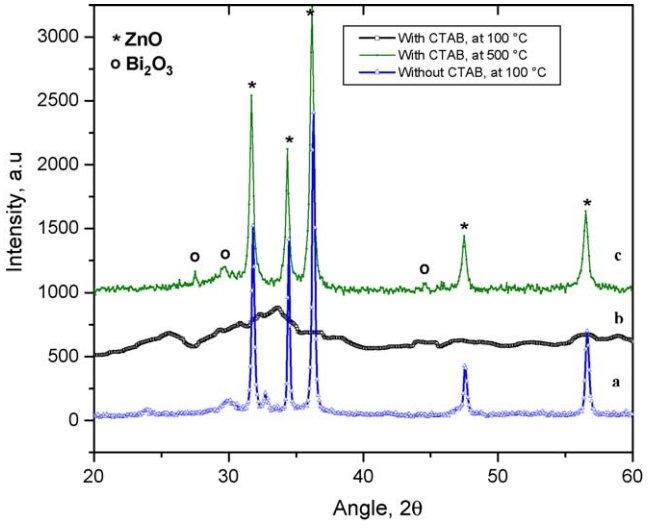

Fig. 1. X-ray diffraction analysis of varistor nanopowder (a) without CTAB at 100 °C, (b) with CTAB at 100 °C, and (c) with CTAB, calcined at 500 °C.

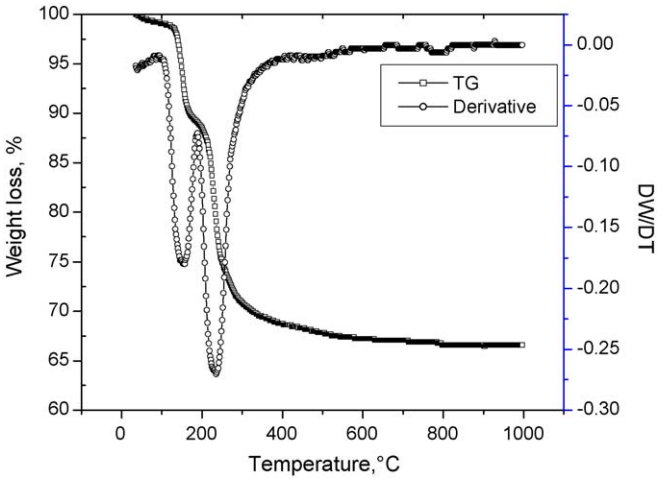

Fig. 2. TG analysis of varistor nanopowder prepared using CTAB.

crystal growth, morphology, particle size distribution, porosity and surface area. In CTAB modified ZnO varistor samples, a crystallite size of 16 nm is obtained even after calcination of the precursor at 500 °C, while that for the directly formed counter part is 24 nm. The TEM micrographs of the varistor grade nanopowder are presented in Fig. 3. Cylindrical rod shaped particles with physical dimensions 500 nm length and 75 nm diameters can be evident in the 'CTAB-free' varistor nanopowders. Growth of nanorods have been extensively reported in simple reflux synthesis and arises from the charge imbalance between the positively charged reactive Zn-(0 0 0 1) surface and the negatively charged O-(0 0 0 1) inert surface [16,20]. The rod shaped varistor nanopowders will result in poor packing during compaction, making it difficult to obtain dense varistors at low temperatures. Surfactants are usually added to reorient the particle growth and are widely employed to obtain spherical morphologies. Here the CTAB added nanopowders exhibit loosely adhered spherical nanoclusters under TEM (Fig. 3b).

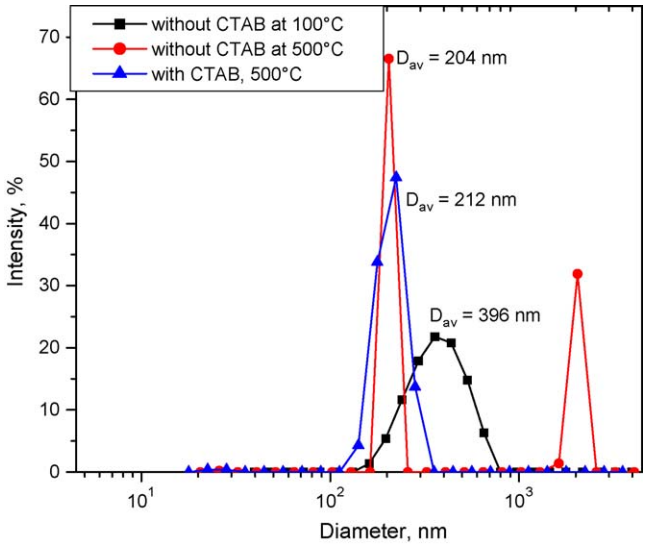

Fig. 4. Particle size distribution analysis of varistor nanopowder, prepared without CTAB at 100 °C, without CTAB calcined at 500 °C and with CTAB calcined at 500 °C.

Such nanoparticles must possess high specific surface area. The BET surface area obtained for the CTAB modified varistor nanopowders was 30 m^2/g and that obtained for CTAB-free powder was only 18 m^2/g. Porosity is also created during the thermal decomposition of CTAB molecules. The advantage over particle size distribution can be confirmed from the particle size analysis given in Fig. 4. The powders prepared without CTAB possessed a wide mono modal size distribution (100 nm to 1 μm) under the as-prepared conditions. Since the CTAB added samples were subjected to calcination, the CTAB-free powder was also calcined at 500 °C prior to particle size analysis for better comparison. After calcination, the powders prepared without CTAB showed a bi-model size distribution with ~70% of particles in the range 204 nm and the remaining around 1 μm.

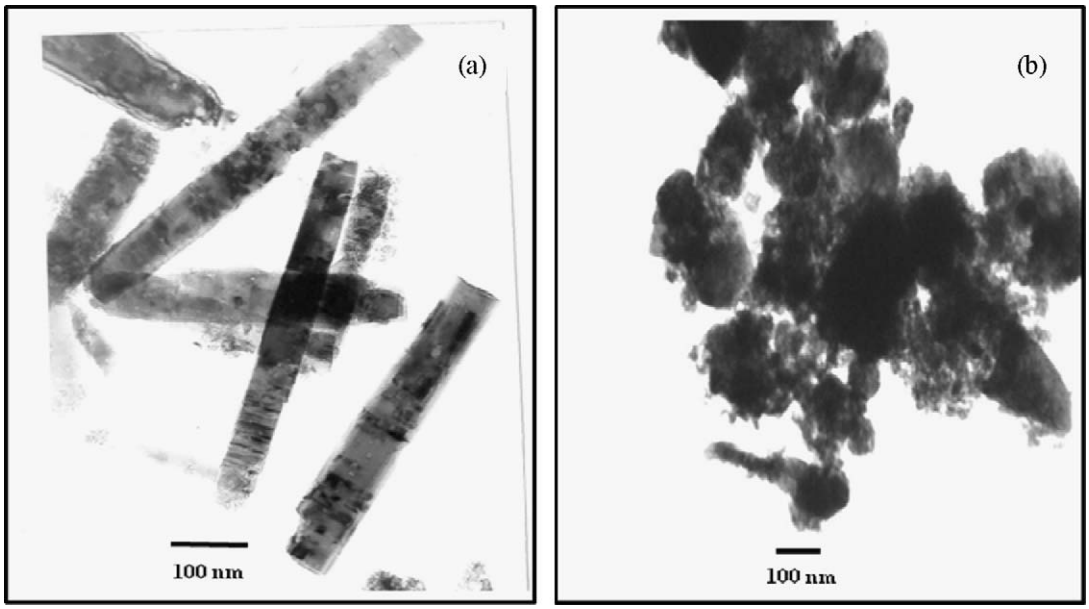

Fig. 3. TEM image of (a) varistor powder refluxed without CTAB and (b) with CTAB.

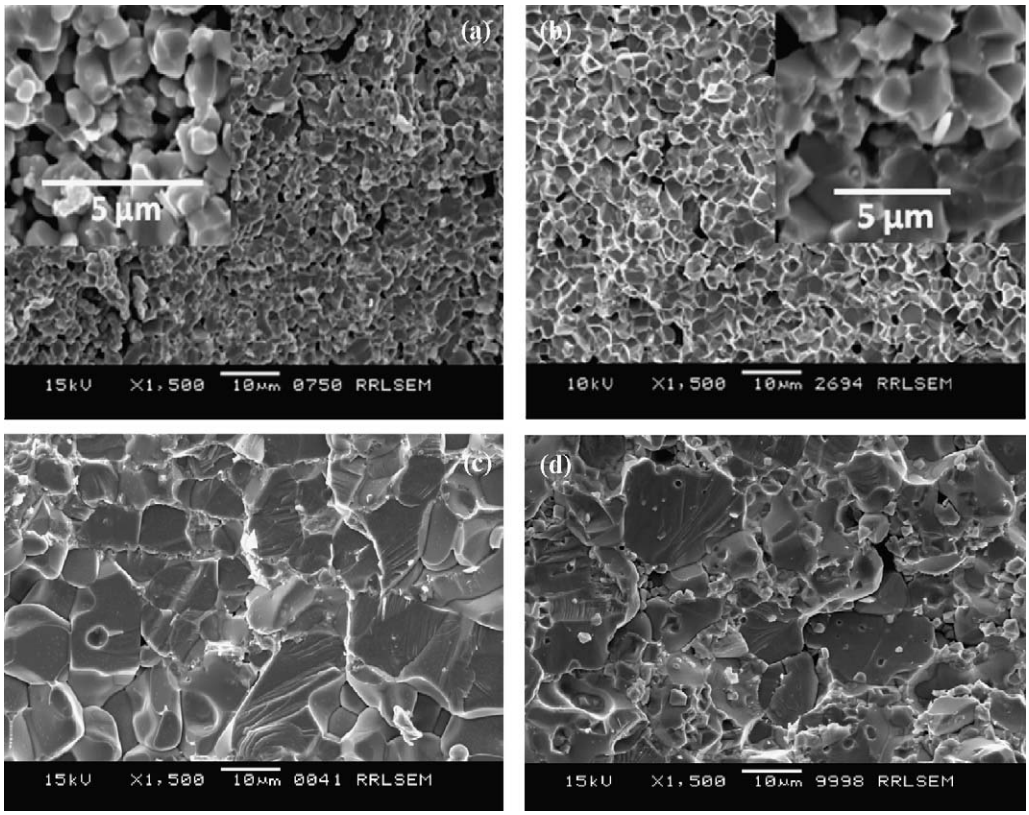

Fig. 5. SEM image of normally sintered varistor samples (a) WS 850, (b) WOS 850, (c) WS 1100, and (d) WOS 1100. Inset of (a) magnified image of WS 850 and (b) magnified image of WOS 850.

On the other hand, the CTAB modified samples possess a narrow size distribution about 212 nm.

3.2. Sintering of surfactant modified varistor nanopowder

Densification of varistors is achieved by liquid phase sintering and the presence of Bi_2O_3 additive produces Bi-rich viscous glassy phase at ~740 °C. However the complete densification close to theoretical density is usually accomplished by ZnO grain growth at sintering temperatures above 1200 °C, performed with intermediate soaking and slow cooling. The sintering process between 800 and 900 °C is very critical due to the enhanced sintering kinetics for diffusion and mass transport followed by grain growth in this region. In fact the growth kinetics further enhanced in nano-origin powders due to its high surface area. 'Constrained-sintering' and 'rate controlled sintering' have been successfully employed for the densification of varistor nanopowders without grain growth [21]. Alternately, rapid heating rates and extended period of aging at low temperatures can produce desired insulating grain boundaries along with the controlled grain growth. Therefore we have opted for the microwave and step-sintering techniques in this study. A heating rate as high as 200 °C/min can be easily achieved in microwave sintering. In two-stage step-sintering the samples are rapidly heated to high temperatures but a prolonged aging is carried out at low temperatures. Here, a peak temperature of 1100 °C and an aging temperature of 850 °C were used. The aging temperature is slightly above the liquid phase formation temperature, ideal for controlling the grain growth and Bi_2O_3 vaporization.

The SEM images in Fig. 5a–d present the microstructures of the solid-state sintered varistor samples prepared with and without CTAB and densified at 850 and 1100 °C, respectively. Fig. 5a and b represents the microstructures of the samples sintered at 850 °C. The SEM image clearly shows the initiation of ZnO grain growth at 850 °C. The samples prepared with CTAB have grown comparatively less and the average grain size determined was 800 nm. In the case of CTAB-free samples this was about 2.5 μm. The sintered densities of the samples were 82% and 65% of TD, respectively. In both cases, the presence of porosity confirms the poor densification. When the sintering temperature was increased to 1100 °C, the theoretical densities increased rapidly and the samples modified with CTAB attained 96.79% sintered density whereas the CTAB-free samples could achieve only 93.93%. The average grain size of these samples was determined as 8 and 10 μm, respectively. The advantage of using CTAB is evident from the uniform distribution of ZnO grains.

Fig. 6a and b shows the SEM images of the samples sintered using microwave. In this case, ZnO grain morphology changed slightly from hexagonal to spherical and in presence of CTAB, the excessive growth reduced appreciably (Fig. 6a and b). The SEM images clearly show the advantages of the rapid heating rates in microwave heating. The molecular level influence of the microwave heating in diffusion assisted grain growth may prevent the excessive growth of ZnO grains. Here also the addition of surfactant ensures more uniform distribution of ZnO

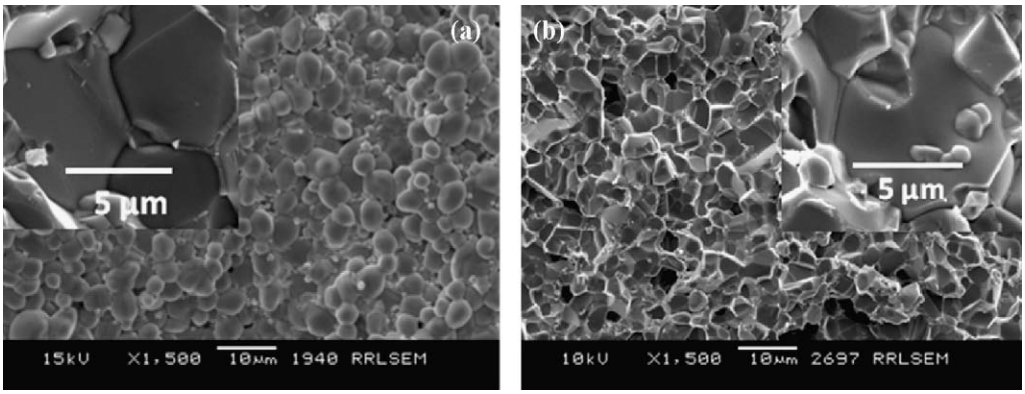

Fig. 6. SEM image of microwave sintered varistor samples (a) WMS and (b) WOMS. Inset of (a) magnified image of WMS and (b) magnified image of WOMS.

grain throughout the varistor volume. The surfactant added samples have homogeneous distribution of ZnO grains and grain boundaries (Fig. 6b). The average ZnO grain size in the order of 6 μm was obtained for both CTAB added and free samples. The CTAB advantage can be seen in the densities of the step-sintered samples. The microwave sintered, CTAB added samples had a theoretical sintered density of 99.75% TD whereas the CTAB-free samples had only 89.29% TD. CTAB is a highly polar organic surfactant that readily absorbs microwaves. The rapid interaction of microwaves with the CTAB molecules produces high degree of dielectric heating at the molecular level resulting in less grown and dense varistors.

The microstructure of step-sintered samples are presented in Fig. 7a and b. The average ZnO grain size of these samples was only 2 μm, irrespective of CTAB addition. The combined effect of microwave sintering and surfactant addition in modifying the grain size and grain distribution is clear from the magnified image given as inset in Fig. 7a. As seen from the magnified images, inset in Fig. 7b, the samples without CTAB have no microstructural uniformity. The microstructure clearly shows the presence of porosities in the CTAB-free samples. The presence of CTAB facilitates uniform particle size distribution and increased particle packing. Moreover, CTAB addition favors the homogeneous distribution of low level varistor dopants that also contribute to densification.

The *I–V* properties of the sintered ZnO samples prepared with and without CTAB are presented in Fig. 8. The change in the average grain size, density and electrical properties of the varistor with respect to the different sintering conditions are also summarized in Table 2. Since all the three modes of sintering resulted in different densities, grain sizes and grain boundary thicknesses, the V_b and 'α' values vary largely. The step-sintered samples show the maximum V_b value obtained is 465 ± 3 V/mm. Even though microwave sintering resulted in the highest theoretical density, the V_b value achieved is only 240 ± 8 V/mm. The solid-state sintered samples have reasonable V_b value, 323 ± 7 V/mm, in spite of the larger grain size. The samples sintered at 850 °C through solid-state route behaved as an ohmic device. In microwave sintered samples, the rapid heating rates may have resulted in the heterogeneous vaporization of low level additives, particularly Bi, causing the reduction in the break down field. In light of this study, we propose rapid microwave heating followed by conventional aging near to liquid phase temperature as appropriate for obtaining desired nano-grained ZnO varistor microstructures. The *I–V* measurements made on CTAB added varistor samples confirm that the V_b value is significantly improved irrespective of the sintering methods. The V_b values obtained in this work are 388, 532 and 246 V/mm for the conventional solid-state, step and microwave sintered samples, respectively. The advantage of CTAB is found in terms of ZnO grain size control and homogeneous distribution of grain boundary additives. In all cases the CTAB added samples showed good non-linear properties.

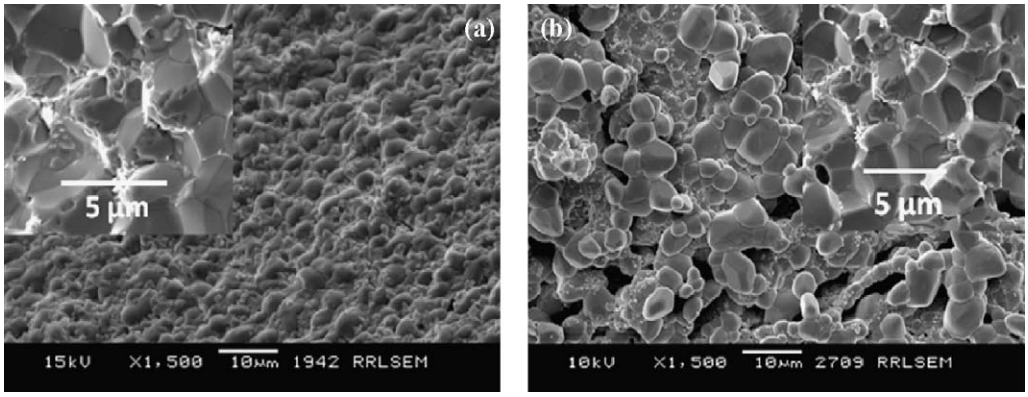

Fig. 7. SEM image of step-sintered varistor samples (a) WSS and (b) WOSS. Inset of (a) magnified image of WSS and (b) magnified image of WOSS.

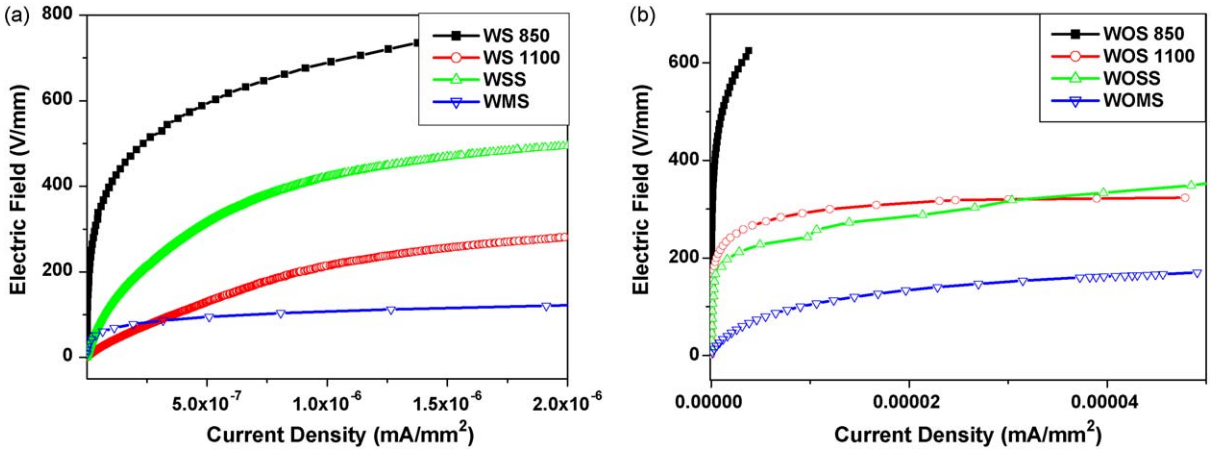

Fig. 8. The current–voltage behavior of the sintered varistor blocks (a) with CTAB and (b) without CTAB.

Table 2
Change in the average grain size, density and electrical properties of the varistor with respect to the different sintering conditions.

Sample	Average grain size (μm)	% Density (g/cm^3)	V_b (V/mm)	Non-linearity coefficient (α)
WS 850	<1	82.86	–	–
WOS 850	>1	65.71	–	–
WS 1100	6	96.79	388	13.28
WOS 1100	10	93.93	323	16.84
WSS	2	93.21	532	7.67
WOSS	3	91.07	465	6.60
WMS	6	99.75	246	17.07
WOMS	7	89.29	240	16.02

4. Conclusions

An attempt on synthesis and sintering characteristics of nano-origin ZnO–Bi_2O_3 varistors has been made. The following conclusions could be made from this work.

1. High surface area nanocrystalline varistor particles can be easily prepared in bulk quantities through reflux reaction involving CTAB surfactant.
2. Among the selected sintering techniques, the microwave sintering resulted in 99% theoretical sintered density with a grain size of 6 μm. The step-sintering resulted in 93% sintered density but having a grain size of only 2 μm. Hence it is proposed to have rapid heating of varistor discs under microwaves and low temperature aging by step-sintering to obtain nano-grained ZnO–Bi_2O_3 varistors.
3. Varistor discs prepared from CTAB modified nano-origin varistor powders show enhanced densification, significant ZnO grain size control and uniform distribution of varistor additives in all the three modes of sintering.
4. In all the cases of sintering, CTAB modified nano-origin varistor discs have shown enhanced breakdown field and high non-linearity.

References

[1] L. Wang, G. Tang, Z.-K. Xu, Preparation and electrical properties of multilayer ZnO varistors with water-based tape casting, Ceram. Int. 35 (2009) 487–492.
[2] S.-T. Kuo, W.-H. Tuan, Y.-W. Lao, C.-K. Wen, H.-R. Chen, Grain growth behavior of Bi_2O_3-doped ZnO grains in a multilayer varistor, J. Am. Ceram. Soc. 91 (2008) 1572–1579.
[3] S.C. Pillai, J.M. Kelly, D.E. McCormack, R. Ramesh, High performance ZnO varistors prepared from nanocrystalline precursors for miniaturized electronic devices, J. Mater. Chem. 18 (2008) 3926–3932.
[4] A.M. Hashimov, S.M. Hasanli, R.N. Mehtizadeh, K.B. Bayramov, S.M. Azizoya, Zinc oxide-and polymer-based composite varistors, Phys. Stat. Sol. C 3 (2006) 2871–2875.
[5] M. Peiteado, J.F. Fernandez, A.C. Caballero, Varistors based in the ZnO–Bi_2O_3 system: microstructure control and properties, J. Eur. Ceram. Soc. 27 (2007) 3867–3872.
[6] S.-Y. Chu, T.-M. Yan, S.-L. Chen, Analysis of ZnO varistors prepared by the sol–gel method, Ceram. Int. 26 (2000) 733–737.
[7] Y.W. Lao, S.T. Kuo, W.H. Tuan, Influence of ball milling on the sintering behavior of ZnO powder, Ceram. Int. 35 (2009) 1317–1320.
[8] P. Duran, J. Tartaj, C. Moure, Fully dense, fine-grained, doped zinc oxide varistors with improved nonlinear properties by thermal processing optimization, J. Am. Ceram. Soc. 86 (2003) 1326–1329.
[9] Suresh C. Pillai, J.M. Kelly, D.E. McCormack, P. O'Brien, R. Ramesh, The effect of processing conditions on varistors prepared from nanocrystalline ZnO, J. Mater. Chem. 13 (2003) 2586–2590.
[10] Y.K. Li, G.R. Li, Q.R. Yin, Preparation of ZnO varistors by solution nano coating technique, Mater. Sci. Eng. B 130 (2006) 264–268.
[11] R. Subasri, M. Asha, K. Hembram, G.V.N. Rao, T.N. Rao, Microwave sintering of doped nanocrystalline ZnO and characterization for varistor applications, Mater. Chem. Phys. 115 (2009) 677–684.
[12] P. Duran, F. Capel, J. Tartaj, C. Moure, Sintering behavior and electrical properties of nanosized doped-ZnO powders produced by metallorganic polymeric processing, J. Am. Ceram. Soc. 84 (2001) 1661–1668.
[13] F. Yuan, H. Ryu, Microstructure of varistors prepared with zinc oxide nanoparticles coated with Bi_2O_3, J. Am. Ceram. Soc. 87 (2004) 736–738.

[14] L.S. Macary, M.L. Kahn, C. Estournes, P. Fau, D. Tremouilles, M. Bafleur, P. Renaud, B. Chaudret, Size effect on properties of varistors made from zinc oxide nanoparticles through low temperature spark plasma sintering, Adv. Funct. Mater. 19 (2009) 1775–1783.

[15] M. Mazaheri, S.A. Hassanzadeh-Tabrizi, S.K. Sadrnezhaad, Hot pressing of nanocrystalline zinc oxide compacts: densification and grain growth during sintering, Ceram. Int. 35 (2009) 991–995.

[16] S. Anas, R.V. Mangalaraja, P. Mukundan, S.K. Shukla, S. Ananthakumar, Direct synthesis of varistor-grade doped nanocrystalline ZnO and its densification through a step-sintering technique, Acta Mater. 55 (2007) 5792–5801.

[17] L. Vayssieres, K. Keis, A. Hagfeldt, S.-E. Lindquist, Three-dimensional array of highly oriented crystalline ZnO microtubes, Chem. Mater. 13 (2001) 4395–4398.

[18] Y. Liu, Y. Chu, L.-L. Li, L.-H. Dong, Y.-J. Zhuo, Controlled fabrication of highly oriented ZnO microrod/microtube arrays on a Zinc substrate and their photoluminescence properties, Chem. Eur. J. 13 (2007) 6667–6673.

[19] Y.D. Wang, S. Zhang, C.L. Ma, H.D. Li, Synthesis and room temperature photoluminescence of ZnO/CTAB ordered layered nanocomposite with flake-like architecture, J. Lumin. 126 (2007) 661–664.

[20] M.Y. Ge, H.P. Wu, L. Niu, J.F. Liu, S.Y. Chen, P.Y. Shen, Y.W. Zeng, Y.W. Wang, G.Q. Zhang, J.Z. Jiang, Nanostructured ZnO: from monodisperse nanoparticles to nanorods, J. Cryst. Growth 305 (2007) 162–166.

[21] M. Peiteado, J.F. Fernandez, A.C. Caballero, Processing strategies to control grain growth in ZnO based varistors, J. Eur. Ceram. Soc. 25 (2005) 2999–3003.